Received: 29 December 2018 | Revised: 7 May 2019 | Accepted: 25 May 2019

DOI: 10.1111/bph.14759

RESEARCH PAPER

MicroRNA-29b-3p reduces intestinal ischaemia/reperfusion injury via targeting of TNF receptor-associated factor 3

Yan Dai[1] | Zhang Mao[1] | Xu Han[1] | Youwei Xu[1] | Lina Xu[1] | Lianhong Yin[1] | Yan Qi[1] | Jinyong Peng[1,2,3]

[1] College of Pharmacy, Dalian Medical University, Dalian, China

[2] Key Laboratory for Basic and Applied Research on Pharmacodynamic Substances of Traditional Chinese Medicine of Liaoning Province, Dalian Medical University, Dalian, China

[3] National-Local Joint Engineering Research Center for Drug Development (R&D) of Neurodegenerative Diseases, Dalian Medical University, Dalian, China

Correspondence
Jinyong Peng, College of Pharmacy, Dalian Medical University, Western 9 Lvshunnan Road, Dalian 116044, China.
Email: jinyongpeng2008@126.com

Funding information
Project of Leading Talents of Dalian, and Liao-Ning Revitalization Talents Program, Grant/Award Number: XLYC1802121; Science and Technology Innovation Project of Dalian, China, Grant/Award Number: 2018J128N083; Key Research and Development Project of Liaoning Province, Grant/Award Number: 2017225090; National Natural Science Foundation of China, Grant/Award Number: 81872921

Background and Purpose: The microRNA miR-29b-3p shows important roles in regulating apoptosis and inflammation. However, its effects on intestinal ischaemia/reperfusion (II/R) injury have not been reported. Here we have investigated the functions of miR-29b-3p on II/R injury on order to find drug targets to treat the injury.

Experimental Approach: Two models - in vitro hypoxia/reoxygenation (H/R) of IEC-6 cells; in vivo, II/R injury in C57BL/6 mice were used. Western blotting and dual-luciferase reporter assays were used and mimic and siRNA transfection tests were applied to assess the effects of miR-29b-3p on II/R injury via targeting TNF receptor-associated factor 3 (TRAF3).

Key Results: The H/R procedure decreased cell viability and promoted inflammation and apoptosis in IEC-6 cells, and the II/R procedure also promoted intestinal inflammation and apoptosis in mice. Expression levels of miR-29b-3p were decreased in H/R-induced cells and II/R-induced intestinal tissues of mice compared with control group or sham group, which directly targeted TRAF3. Decreased miR-29b-3p level markedly increased TRAF3 expression via activating TGF-α-activated kinase 1 phosphorylation, increasing NF-κB (p65) levels to promote inflammation, up-regulating Bcl2-associated X expression, and down-regulating Bcl-2 expression to trigger apoptosis. In addition, the miR-29b-3p mimetic and TRAF3 siRNA in IEC-6 cells markedly suppressed apoptosis and inflammation to alleviate II/R injury via inhibiting TRAF3 signallimg.

Conclusions and Implications: The miR-29b-3p played a critical role in II/R injury, via targeting TRAF3, which should be considered as a significant drug target to treat the disease.

1 | INTRODUCTION

Intestinal ischaemia/reperfusion (II/R) injury is closely related to mesenteric ischaemia, haemorrhagic shock, and organ transplantation (Enyindah-Asonye et al., 2017; X. H. Liu et al., 2015; Matsuo, Chaung, Liou, Wang, & Yang, 2018; W. Zhou et al., 2017). Intestinal ischaemia can cause cell damage and provoke epithelial barrier dysfunction during reperfusion, resulting in systemic inflammatory response syndrome (SIRS), multiple organ dysfunction syndrome (MODS), and death (Duranti et al., 2018; Feng et al., 2017; Impellizzeri et al., 2016). Thus, exploration of possible drug targets for the prevention and treatment of II/R injury is necessary.

Abbreviations: H&E, haematoxylin–eosin; H/R, hypoxia/reoxygenation; II/R, intestinal ischaemia/reperfusion; MODS, multiple organ dysfunction syndrome; NC, negative control; SIRS, systemic inflammatory response syndrome; TAK1, TGF-α-activated kinase 1; TRAF3, TNF receptor-associated factor 3.

Previous studies have reported that inflammation, oxidative stress, and cell apoptosis are associated with II/R injury. Reperfusion of ischaemic areas of intestine can cause the release of pro-inflammatory mediators and reinforce the injury (Feng et al., 2017). Excessive ROS can cause cell apoptosis, destroy intestinal epithelial homeostasis, and induce cell death (Filpa et al., 2017). Many groups have shown that cell apoptosis is one major mode of cell death caused by II/R (Ikeda et al., 1998; Y. Li, Wen, et al., 2017; Y. Li, Xu, et al., 2017; Wen et al., 2012), and uncontrolled inflammatory response is an important mechanism to cause SIRS. Thus, exploration of drug targets in inhibiting inflammation and apoptosis is very important to mitigate II/R injury.

MicroRNAs (miRNAs) are important endogenous regulators leading to RNA degradation and/or inhibition of protein synthesis (He et al., 2018; Y. Hu et al., 2018; Z. Liu et al., 2016). Recent studies have shown that some miRNAs including miR-378, miR-351-5P, and miR-665-3p play important roles in regulating II/R injury (Y. Hu et al., 2018; Z. Li et al., 2018; Y. Li, Wen, et al., 2017 ; Y. Li, Xu, et al., 2017). MiR-378 can protect against II/R injury via inhibiting intestinal mucosal cell apoptosis (Y. Li, Wen, et al., 2017; Y. Li, Xu, et al., 2017). Inhibition of miR-351-5p can alleviate II/R-induced intestinal oxidative stress, inflammation, and apoptosis via targeting MAPK13 and sirtuin-6 (Y. Hu et al., 2018). Inhibition of miR-665-3p can inhibit inflammation and apoptosis in II/R via targeting the autophagy-related gene 4B (Z. Li et al., 2018). Thus, exploration of novel miRNAs which are able to diminish II/R injury is important in developing drug targets.

The miRNA miR-29b belongs to the miR-29 family, comprising miR-29a, miR-29b, and miR-29c. Recent studies have revealed that miR-29b plays important roles in a variety of diseases (Langsch et al., 2016; S. Zhou et al., 2018). This miRNA can prevent doxorubicin-induced myocardial apoptosis by targeting **BAX** (Jing, Yang, Jiang, Chen, & Wang, 2018), inhibit high-mobility group box 1/**TLR4** signallling in liver fibrosis (Zhang et al., 2017), inhibit breast cancer via targeting the DNA modifying enzyme TET1 (H. Wang et al., 2017), and alleviate IgAN pathogenesis via targeting the **cyclin-dependent kinase 6** (Xing et al., 2014). However, there are no reports of the effects of miR-29b-3p on II/R injury.

The TNF receptor-associated factor (TRAF) family contains seven members in mammals (Inoue et al., 2000), in which TRAF3 is a crucial signal transducer in IFN regulatory factor, NF-κB, and apoptotic signal pathways (J. Hu et al., 2016; Qu, Xiang, Zhou, Qin, & Yu, 2017). TRAF3, ubiquitously expressed in brain, lung, heart, spleen, and liver, is the target gene of some miRNAs including miR-322, miR-455, and miR-214 (Gu et al., 2015; Rehei et al., 2018; Yao, Tang, Li, Fan, & Cao, 2016). Overexpression of miR-322 can ameliorate high glucose-induced injury on neural stem cells via targeting TRAF3 (Gu et al., 2015). MiR-455 can inhibit neuronal cell death by inhibiting TRAF3 in cerebral ischaemic stroke (Yao et al., 2016). Depression of miR-214 can significantly restrain osteosarcoma cell invasion and migration via targeting TRAF3 (Rehei et al., 2018). However, the roles of TRAF3 on II/R injury remain unknown. In addition, the effects of miR-29b-3p on II/R injury via targeting TRAF3 have not been reported.

What is already known

- MiR-29b-3p plays important roles in apoptosis and inflammation.

What this study adds

- MiRNA-29b-3p decreases intestinal ischaemia/reperfusion injury through suppressing apoptosis and inflammation by targeting TRAF3.

What is the clinical significance

- MiR-29b-3p/TRAF3 signalling is a potential drug target for clinical diagnosis and treatment of intestinal ischaemia/reperfusion injury.

Thus, the aim of the present work was to investigate the molecular mechanisms of miR-29b-3p on II/R injury by targeting TRAF3, in order to identify possible drug targets to prevent and treat the injury.

2 | METHODS

2.1 | Cell culture and hypoxia/reoxygenation model

Rat intestinal epithelial IEC-6 cells (RRID:CVCL_0343) obtained from Shanghai Institutes for Biological Sciences (Shanghai, China) were cultured in an atmosphere containing 5% CO_2 and 21% O_2 at 37°C with DMEM (Gibco, CA, USA) which supplemented with 1% penicillin/streptomycin and 10% FBS. Culture medium was replaced every 2 or 3 days in all experiments. IEC-6 cells incubated in PBS were transferred to an incubator (Thermo Fisher Scientific, Inc., USA) containing 5% CO_2 and 1% O_2 balanced with 94% N_2 at 37°C for 4 hr. Then the cells were cultured under normal conditions for 0, 120, 720, and 1,440 min to achieve reoxygenation. The cells in the control group received the same treatment as the cells in hypoxia/reoxygenation (H/R) group except that the culture condition was controlled by an incubator (NUAIR, USA) with 5% CO_2 and 21% O_2 at 37°C. Cell viability and morphology of each control group were the same, and therefore, results from only one control group are given in the present work.

2.2 | Cell viability assay

IEC-6 cells were inoculated into 96-well plates at a density of 5–10 × 10^4 cells·ml^{-1}, and H/R experiments were carried out on the next day (n = 6); 15 μl of MTT solution (5 mg·ml^{-1}) was added to every well at the end of H/R process. After 4 hr of incubation at 37°C under light avoidance condition, the medium was replaced by 150 μl of DMSO, and the OD value at 490 nm was recorded using a POLARstar OPTIMA multi-detection microplate reader (BioRad, San Diego, CA, USA).

2.3 | Animals and II/R-induced intestinal injury model

All animal care and experimental procedures were carried out in accordance with People's Republic of China Legislation Regarding the Use and Care of Laboratory Animals and approved by the Animal Care and Use Committee of Dalian Medical University. Animal studies are reported in compliance with the ARRIVE guidelines (Kilkenny, Browne, Cuthill, Emerson, & Altman, 2010; McGrath & Lilley, 2015). All animal studies complied with the principles of Replacement, Refinement, or Reduction (the 3Rs).

Forty male C57BL/6J mice (RRID:IMSR_JAX:000664) weighing 18–22 g (6–8 weeks old) were supplied by the Experimental Animal Center at Dalian Medical University, Dalian, China (SCKK: 2018-0003), All animals were group-housed with two to three mice per cage on a 12-hr light/dark cycle in a temperature-controlled (25 ± 2°C) room with free access to water and food. Before the experiment, all mice were fasted for 24 hr, but the water was supplied. The animals were anaesthetized with intraperitoneal injecting 1.0–1.25 $g{\cdot}kg^{-1}$ of 10% urethane in 0.9% saline (w/v; Sigma-Aldrich, USA), and all mice were kept under anaesthesia during the periods of surgery.

The mice were randomly divided into five groups (n = 8): sham group and II/R groups (45 min of ischaemia and reperfusion for 30, 90, 720, and 1,440 min). In the sham group, the wound was closed after finding the superior mesenteric artery by laparotomy. In II/R groups, the abdominal cavity was opened, superior mesenteric artery and its adjacent tissues were cautiously isolated and clamped with a microvascular clip for 45 min to cause ischaemia, and then the clip was gently removed to allow reperfusion for 30, 90, 720, and 1,440 min. After the procedure, the surgical incision was closed with sutures. During the process, the mice were placed on a warming plate and killed after the injury. Then the whole intestine was removed and stored at −80°C, until were used for assays.

2.4 | Histopathological examination

Intestinal tissues of mice were fixed by 4% paraformaldehyde, embedded in paraffin, cut into sections (5-μm thick) and stained with haematoxylin & eosin (H&E). Images of the stained sections were obtained using a light microscope (Nikon Eclipse TE2000-U, Japan) with 200× magnification. II/R-induced mucosal injury was evaluated according to the Chiu's score. Injury was scored in a blinded fashion from 0 to 5 on a scale based on the method described by Feinman et al. (2010) and Tackett, Gandotra, Bamdad, Muise, & Cowles (2019). The experimenters were blinded to the treatments given to each group of animals (n = 8).

2.5 | TUNEL assay

TUNEL assays used the assay kit (Beijing TransGen Biotech Co., Ltd., China) following the manufacturer's instructions. In vivo, the paraffin tissue sections were dewaxed with xylene and washed with PBS. Then the tissue samples were permeated with 0.5% Triton-100 and incubated with 50 μl of TUNEL reaction mixture for 1 hr at 37°C under light avoidance and humid conditions. Finally, the tissue sections were washed with PBS, permeated with 0.5% Triton-100, and closed with cover glass. In vitro, H/R-treated IEC-6 cells in 24-well plates were washed with PBS, fixed with 4% paraformaldehyde for 20 min, and permeated with 0.5% Triton-100. Then 150 μl of TUNEL reaction mixture was added into the plates for 1 hr at 37°C under light avoidance. Finally, the images were captured by a fluorescent microscopy (Olympus, Japan) with 200× magnification and analysed by the ImageJ Software (National Institutes of Health, USA). The counting of the cells was carried out in a blinded fashion.

2.6 | Detection of miR-29b-3p levels in vivo and vitro

Total miRNA samples were extracted from intestinal tissues and IEC-6 cells using SanPrep Column MicroRNA Mini-Preps Kit according to the manufacturer's protocol. The purity of the extracted miRNA was determined using Micronucleic Acid Protein Analyzer (Biochrom, USA), and the RT-PCR was carried out using a microRNA First Strand cDNA Synthesis Kit following the manufacturer's instructions with a TC-512 PCR system (TECHNE, UK). The levels of miR-29b-3p were determined (n = 5) using MicroRNAs Quantitation PCR Kit and ABI 7500 Real Time PCR System (Applied Biosystems, USA) according to the manufacturer's instructions. The primers of miRNAs are given in Table S1. U6 (Sangon Biological Engineering Technology & Services Co., Ltd., China) was used for normalization of miRNAs.

2.7 | Dual-luciferase reporter assay

TRAF3 cDNAs containing the putative (wild-type, TRAF3-WT) or mutated binding site for miR-29b-3p were synthesized and then cloned into a pmiR-report vector. Mutations in miR-29b-3p binding site were generated from 5′-GGTGCTA-3′ to 5′-CCACGAT-3′ (TRAF3-Mut1), 5′-TGGTGCT-3′ to 5′-ACCACGA-3′ (TRAF3-Mut2), or at both binding sites (TRAF3-Mut3). For the assay, IEC-6 cells were co-transfected with miR-29b-3p mimic and TRAF3-WT, miR-29b-3p mimic negative control (NC) and TRAF3-WT, miR-29b-3p mimic and TRAF3-MUT1, miR-29b-3p mimic NC and TRAF3-MUT1, miR-29b-3p mimic and TRAF3-MUT2, miR-29b-3p mimic NC and TRAF3-MUT2, miR-29b-3p mimic and TRAF3-MUT3, and miR-29b-3p mimic NC and TRAF3-MUT3 in 24-well plates. After 24 hr of transfection, the luciferase activity was assessed (n = 5) by the kit using Dual-Light Chemiluminescent Reporter Gene Assay System (Berthold, Germany), which was normalized to firefly luciferase activity.

2.8 | Co-transfection tests of miR-29b-3p mimic and TRAF3 overexpression plasmid

IEC-6 cells were inoculated into six-well plates. The experiments were divided into control group, miR-29b-3p mimic NC and TRAF3

overexpression plasmid NC co-transfection group, TRAF3 overexpression plasmid single transfection group, and miR-29b-3p mimic and TRAF3 overexpression plasmid co-transfection group. Lipofectamine2000 was dissolved in DMEM, and the solution was equilibrated at room temperature for 5 min to produce solution A. MiR-29b-3p mimic (or miR-29b-3p mimic NC; 50 nM) and TRAF3 overexpression plasmid (or TRAF3 overexpression plasmid NC; 400 ng·ml^{-1}) were separately dissolved in DMEM to produce solutions B (or D) and C (or E). Then D and E solutions were mixed with solution A to produce solution F. The solution C was mixed with solution A to produce solution G. B and C solutions were mixed with solution A to produce solution H. F, G, and H solutions were balanced at room temperature for 20 min. IEC-6 cells were transfected with F, G, and H solutions for 5 hr at 37°C and then changed with fresh medium and cultured in normal conditions. After 24 hr of transfection, the mRNA level of TRAF3 was assessed by real-time PCR assay, and the protein level of TRAF3 was also detected by western blotting assay (n = 5).

2.9 | Immunofluorescence assay

The antibody-based procedures used in this study comply with the recommendations made by the *British Journal of Pharmacology*. In vivo, the paraffin tissue sections were dewaxed and blocked with 3% BSA-PBS for 1 hr at room temperature and incubated in one humidified box overnight at 4°C with anti-TRAF3 with 1:100 dilution. On the next day, the samples were incubated with Alexa fluorescein-labelled secondary antibody for 1 hr at 37°C and stained with DAPI (1 μg·ml^{-1}) for 5–10 min in the dark conditions. In vitro, IEC-6 cells were fixed with 4% paraformaldehyde for 20 min after H/R process, and the following steps were performed as the same as tissue sections described above. Finally, a fluorescent microscopy (Olympus, Japan) with 200× magnification was used to capture the images.

2.10 | Quantitative real-time PCR assay

Total RNA samples were extracted from intestine tissues of mice and IEC-6 cells using TransZol, which were then reverse transcribed into cDNA using the kit of TransStart Top Green qPCR SuperMix according to the instructions. qRT-PCR was performed on a CFX96 PCR system (Bio-Rad Laboratories, USA) with SYBR Green Master Mix. The forward (F) and reverse (R) primers of RNA are given in Table S2. The levels of mRNA were normalized to β-actin, and the relative level was analysed using the $2^{-\triangle\triangle Ct}$ method (n = 5).

2.11 | Western blotting assay

Protein samples from intestinal tissues of mice and IEC-6 cells were extracted using RIPA containing protease and phosphatase inhibitors. The protein concentrations of the samples were determined using the assay kit following the manufacturer's protocol. The samples were separated on SDS-PAGE (8–12%) gel, transferred to PVDF membranes (Millipore, USA), blocked with 5% dried skim milk (Boster Biological Technology, China) for 2 hr at room temperature, and incubated with primary antibodies (listed in Table S3) overnight at 4°C. After addition of anti-rabbit or anti-mouse secondary antibody for 2 hr at room temperature, the expression levels of the proteins were detected by enhanced chemiluminescence method, and the results were photographed with a ChemiDoc™XRS Imaging System (Bio-Rad Laboratories, USA). Intensity values of the relative protein levels were normalized to β-actin (n = 5).

2.12 | Mimic transfection of miR-29-3p in vitro

Lipofectamine2000 was diluted with DMEM, which was equilibrated for 5 min at room temperature. In addition, miR-29-3p mimic and mimic NC were separately dissolved in DMEM; 50 nM of miR-29b-3p mimic and its NC as the transfection concentrations were used (Sun et al., 2018; Zheng et al., 2019). Each solution was combined with Lipofectamine2000 transfection reagent according to the manufacturer's protocol. Afterwards, the solution was gently mixed to form liposomes for 20 min. IEC-6 cells transfected with the transfection mixture were maintained for 5 hr at 37°C and then changed with fresh medium and cultured in normal conditions for 24 hr, which were subjected to 4 hr of hypoxia and 120 min of reoxygenation. The items of cell apoptosis, miR-29b-3p expression level, and the mRNA or protein levels of TRAF3, **IL-1β**, **IL-6**, **TNF-α**, TGF-α-activated kinase 1 (**TAK1**), p-TAK1, NF-κB, BAX, and **Bcl-2** were determined.

2.13 | Transfection of TRAF3 siRNA in vitro

TRAF3 siRNA (50 nM) and TRAF3 siRNA NC (50 nM) were separately dissolved in DMEM solution, which were blended with Lipofectamine2000 transfection reagent according to the manufacturer's protocol. The mixed reagents were mixed at room temperature for 20 min to form liposomes. IEC-6 cells were transfected with the transfection mixture. After 24 hr of transfection, cell apoptosis, the mRNA or protein levels of TRAF3, TAK1, p-TAK1, NF-κB, BAX, Bcl-2, IL-1β, IL-6, and TNF-α were detected.

2.14 | Data and statistical analysis

The data and statistical analysis in this study comply with the recommendations on experimental design and analysis in pharmacology (Curtis et al., 2018).The data were expressed as the mean ± *SD*. GraphPad Prism 6.01 software (GraphPad Software, Inc., CA, USA) was used to handle these data and only when a minimum of n = 5 independent samples was acquired. Among them, some data were normalized to control unwanted sources of variation according to following methods. First, the data should be normalized to bring all of the variation into proportion with one another after removing the outliers. Then the coefficients associated with each variable will scale appropriately to adjust for the disparity in the variable sizes. Statistical analysis was performed with one-way ANOVA followed by Tukey's post hoc test when comparing multiple groups, with unpaired t test when

comparing two different groups. Post hoc tests were run only if F achieved $P < .05$ and there was no significant variance inhomogeneity. Statistical significance was considered to be $P < .05$.

2.15 | Materials

3-(4,5-Dimethylthiazol-2-yl)-2,5-diphenyl tetrazolium bromide (MTT) was provided by Roche Diagnostics (Basel, Switzerland). Lipofectamine2000, TransZolTM, TransScript® All-in-One First-Strand cDNA Synthesis SuperMix for qPCR (One-Step gDNA Removal), and TransStart® Top Green qPCR SuperMix were purchased from Beijing TransGen Biotech Co., Ltd. (Beijing, China). SanPrep Column MicroRNA Mini-Preps Kit, MicroRNA First Strand cDNA Synthesis Kit, and MicroRNAs Quantitation PCR Kit were purchased from Sangon Biological Engineering Technology & Services Co., Ltd. (Shanghai, China). Double-Luciferase Reporter Assay Kit was purchased from Promega Biotech Co., Ltd. (Beijing, China). Tissue Protein Extraction Kit was purchased from KEYGEN Biotech. Co., Ltd. (Nanjing, China). The bicinchoninic acid protein assay kit, cell lysis buffer, and PMSF were obtained from Beyotime Institute of Biotechnology (Jiangsu, China). SDS, hydroxymethyl aminomethane (Tris), and DAPI were obtained from Sigma (St. Louis, MO, USA). MiR-29b-3p mimic and TRAF3 (RRID:Addgene_44035) siRNA were purchased from RiboBio. Co., Ltd (Guangzhou, China). TRAF3 plasmids were purchased from GeneCopoeia, Inc. (USA).

2.16 | Nomenclature of targets and ligands

Key protein targets and ligands in this article are hyperlinked to corresponding entries in http://www.guidetopharmacology.org, the common portal for data from the IUPHAR/BPS Guide to PHARMACOLOGY (Harding et al., 2018), and are permanently archived in the Concise Guide to PHARMACOLOGY 2017/18 (Alexander, Kelly, et al., 2017; Alexander, Peters, et al., 2017; Alexander, Striessnig, et al., 2017).

3 | RESULTS

3.1 | H/R and II/R promoted damage in vitro and in vivo

As shown in Figure 1a,b, after 120 min of reoxygenation, the morphology of IEC-6 cells was clearly changed and cell viability was decreased, compared with control group. However, cell morphology and viabilities were improved with the prolongation of reoxygenation time, compared with 120 min of reoxygenation. Meanwhile, as shown in Figure 1c,d, the effects of ischaemia for 45 min and reperfusion for 30, 90, 720, and 1,440 min on intestinal injury in mice were observed. After reperfusion, inflammatory cell infiltration and necrosis were clearly increased in II/R groups, and the most serious injury was found at 90 min of reperfusion. Nevertheless, with the prolongation of

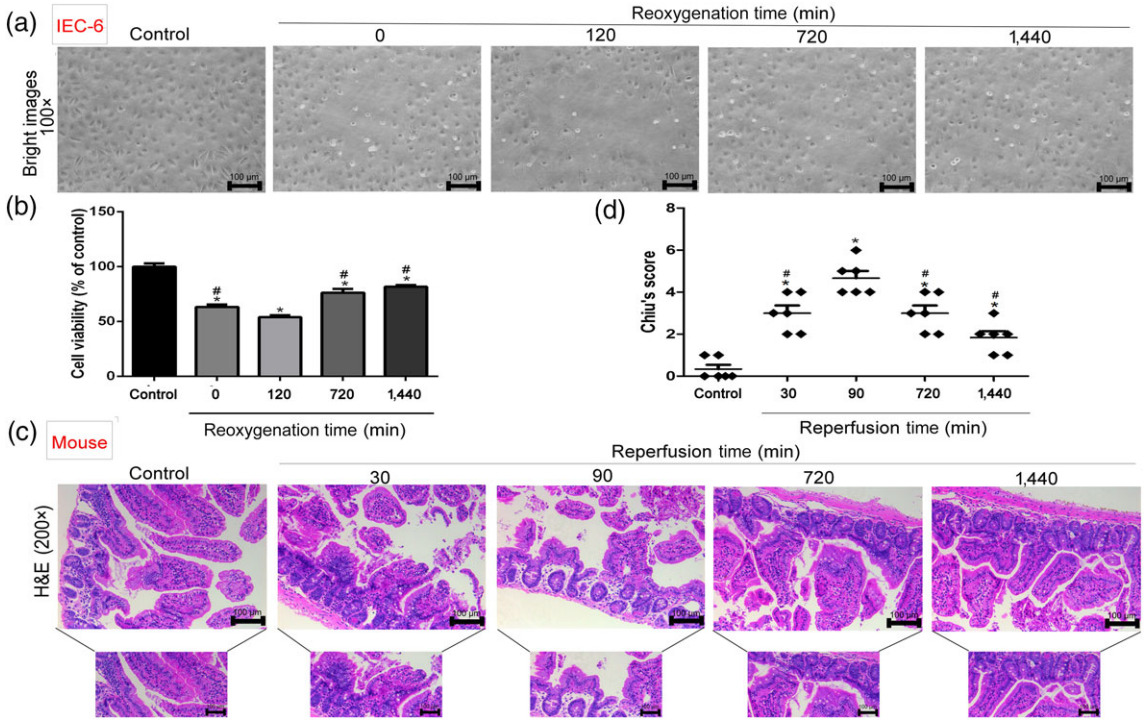

FIGURE 1 H/R injury in IEC-6 cells and II/R damage in mice. (a, b) Cellular morphology and viabilities of IEC-6 cells. After hypoxia for 4 hr and reoxygenation for 0, 120, 720, and 1,440 min, the percentages of viable cells were determined using MTT assay ($n = 6$). (c, d) H&E staining (200× magnification) and histopathological scores (Chiu's score) in mice ($n = 8$). Scale bar = 100 μm. Male C57BL/6 mice were randomly divided into sham group and II/R groups (45 min of ischaemia and reperfusion for 30, 90, 720, and 1,440 min). All data are expressed as the mean ± *SD*. $^{*}P < .05$, significantly different from control groups; $^{\#}P < .05$, significantly different from 120 min of reoxygenation or 90 min of reperfusion group

reperfusion time, the injury was restored compared with 90 min of reperfusion according to Chiu's score and H&E staining.

3.2 | H/R and II/R caused apoptosis in vitro and in vivo

As shown in Figure 2a, the numbers of apoptotic cells were increased in H/R groups compared with control group. However, with the prolongation of reoxygenation time, the numbers of apoptotic cells were reduced compared with 120 min of reoxygenation. The data in Figure 2b showed that the numbers of apoptotic cells were increased in II/R groups compared with sham group, which were gradually reduced with the prolongation of reperfusion time compared with 90 min of reperfusion. The analytical data of the apoptotic cells in vitro and in vivo are shown in Figure 2c,d.

3.3 | TRAF3 is the target gene of miR-29b-3p

The data in Figure 3a showed that after H/R in IEC-6 cells and II/R in mice, the expression levels of miR-29b-3p were significantly decreased with the minimum values at 4 hr of hypoxia and 120 min of reoxygenation in vitro and 45 min of ischaemia and 90 min of reperfusion in vivo compared with control group or sham group. However, the expression levels of miR-29b-3p were clearly increased from 720 to 1,440 min of reoxygenation or reperfusion compared with 120 min of reoxygenation in vitro or 90 min of reperfusion in vivo. The RNA sequence alignment showed that the 3′-UTR of TRAF3 mRNA contained a complementary site for the seed region of miR-29b-3p (Figure 3b). The results in Figure 3c confirmed that the relative luciferase expression in TRAF3-WT + miR-29b-3p mimic group was significantly decreased compared with TRAF3-WT + miR-29b-3p mimic NC group. Compared with TRAF3-MUT1 + miR-29b-3p mimic NC group and TRAF3-MUT2 + miR-29b-3p mimic NC group, the relative luciferase expressions in TRAF3-MUT1 + miR-29b-3p mimic group and TRAF3-MUT2 + miR-29b-3p mimic group were also decreased. However, compared with TRAF3-MUT3 + miR-29b-3p mimic NC group, the relative luciferase expression in TRAF3-MUT3 + miR-29b-3p mimic group showed little change. Therefore, TRAF3 showed specific binding sites with miR-29b-3p. As shown in Figure 3d, the plasmid was TRAF3 overexpression plasmid, and NC referred to TRAF3 overexpression plasmid NC and miR-29b-3p mimic NC. In addition, the results after transfection showed that the expression level of TRAF3 was significantly increased compared with control group, suggesting that TRAF3 overexpression plasmid was successfully transferred into the cells. However, the mRNA level of TRAF3 was obviously decreased in co-transfected TRAF3 overexpression plasmid and

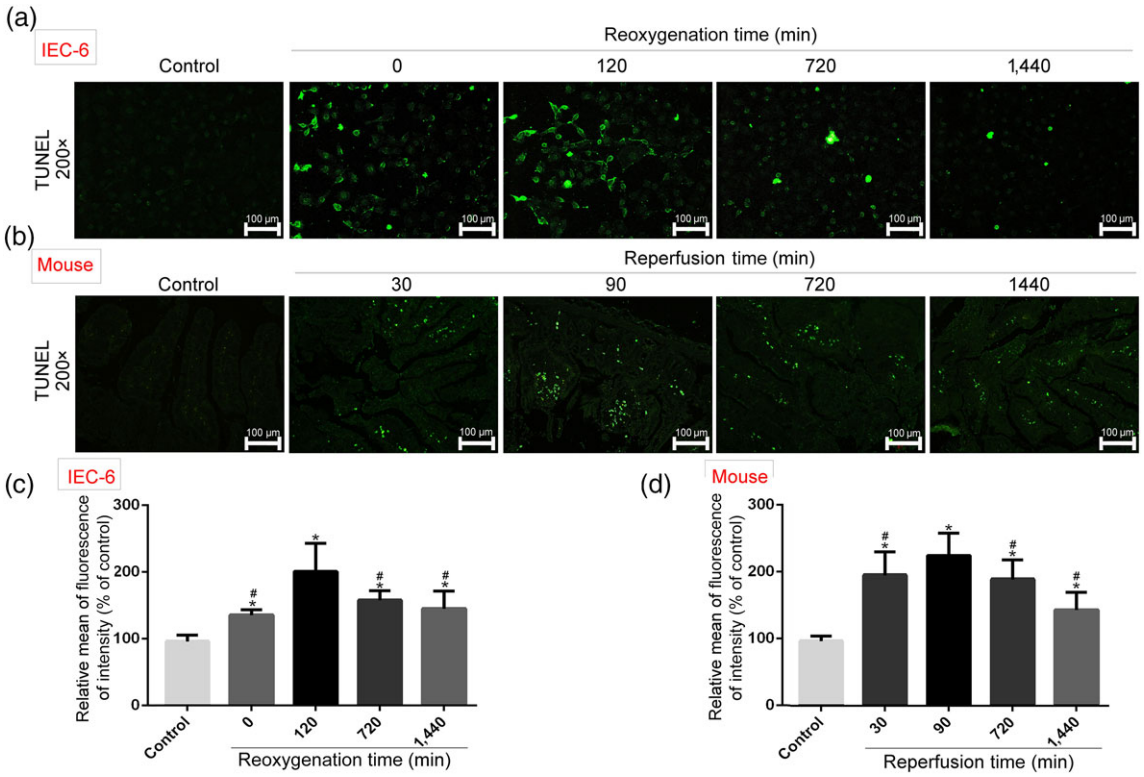

FIGURE 2 Cell apoptosis after H/R in vitro and II/R in vivo. Cell apoptosis was detected based on TUNEL assay. In vitro, IEC-6 cells were incubated in PBS in an incubator containing 5% CO_2, 1% O_2, and 94% N_2 at 37°C for 4 hr. Then the cells were cultured under normal conditions for different times (0, 120, 720, and 1,440 min) to achieve reoxygenation. In vivo, superior mesenteric arteries of mice were carefully clamped with a small vascular clamp for 45 min of ischaemia and reperfusion for different times (30, 90, 720, and 1,440 min). All data are expressed as the mean ± *SD* (n = 5). $^{*}P < .05$, significantly different from control groups; $^{\#}P < .05$, significantly different from 120 min of reoxygenation or 90 min of reperfusion group

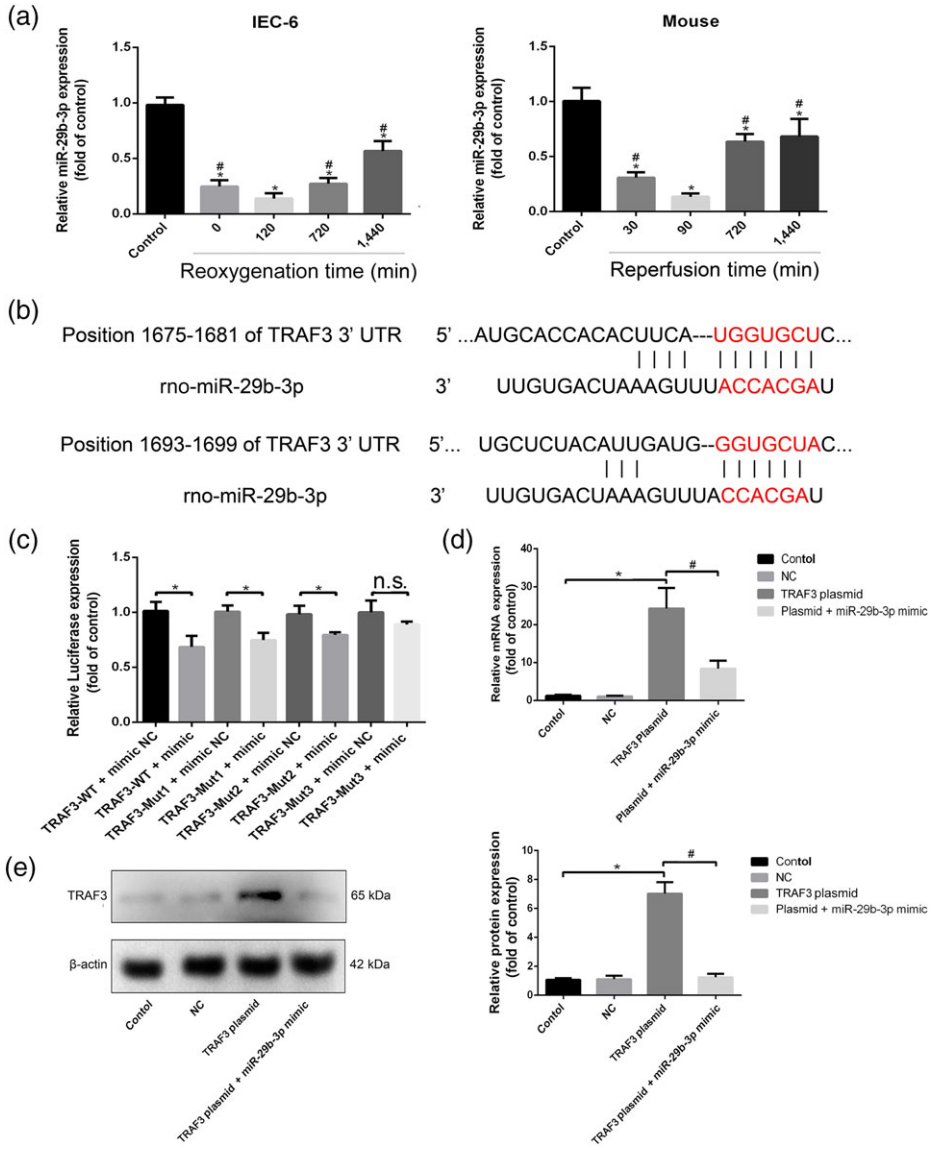

FIGURE 3 TRAF3 is the target gene of miR-29b-3p. (a) The expression levels of miR-29b-3p after H/R injury in IEC-6 cells and II/R injury in mice based on real-time PCR assay. (b) The diagram of miR-29b-3p conservative seed binding sites on the 3′-UTRs of the target genes (TRAF3). (c) Relative luciferase expression with TRAF3 3′-UTR after co-transfected with miR-29b-3p mimic or NC. IEC-6 cells were seeded in 24-well plates and co-transfected with miR-29b-3p mimic or NC and TRAF3-WT or TRAF3-mutant (MUT). After 24 hr of transfection, the luciferase activities were assessed using Dual-Luciferase Reporter Assay Kit. (d, e) The expression levels of TRAF3 after co-transfection. IEC-6 cells were seeded in six-well plates for 24 hr and then co-transfected with miR-29b-3p mimic NC and TRAF3 overexpression plasmid NC, miR-29b-3p mimic and TRAF3 overexpression plasmid, single transfected with TRAF3 overexpression plasmid. Then the mRNA level of TRAF3 was assessed by real-time PCR assay, and the protein level of TRAF3 was detected by western blotting assay after transfection. All data are expressed as the mean ± *SD* (n = 5). $^{*}P$ < .05 compared with control group in Figure 3a,d,e and compared with NC group in Figure 3c; $^{\#}P$ < .05 compared with 120 min of reoxygenation or 90 min of reperfusion group in Figure 3a and compared with TRAF3 plasmid group in Figure 3d,e; n.s., no significance

miR-29b-3p mimic group compared with single transfected TRAF3 overexpression plasmid group, suggesting that miR-29b-3p inhibited TRAF3 expression. The results in Figure 3e showed that compared with control group, the protein level of TRAF3 was significantly increased after transfection of TRAF3 overexpression plasmid. However, compared with co-transfected TRAF3 overexpression plasmid and miR-29b-3p mimic, the expression level of TRAF3 was clearly reduced. To summarize, our data confirmed that TRAF3 is the target gene of miR-29b-3p.

3.4 | H/R and II/R up-regulated the expression levels of TRAF3 in vitro and in vivo

The mRNA levels of TRAF3 are shown in Figure 4a based on real-time PCR assay, and the protein levels of TRAF3 are shown in Figure 4b,c based on immunofluorescence staining and western blotting assay. The mRNA and protein levels of TRAF3 were markedly increased in H/R groups after 4 hr of hypoxia and 120 min of reoxygenation in vitro compared with control group, which were also increased under 45 min

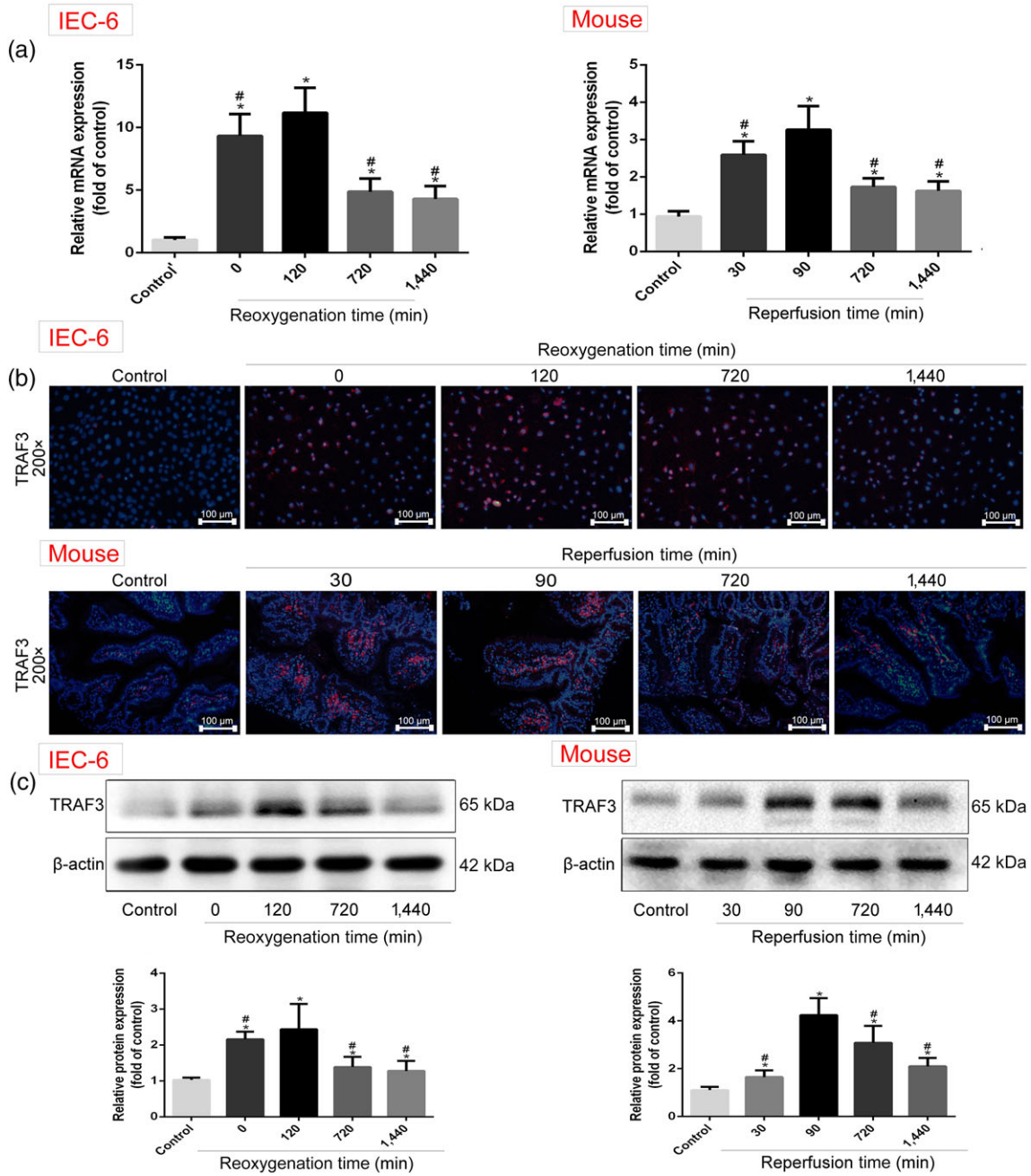

FIGURE 4 TRAF3 expression levels in H/R-caused IEC-6 cells and II/R-caused mice. (a) The mRNA levels of TRAF3 in IEC-6 cells and mice based on real-time PCR assay. (b) The protein levels of TRAF3 in vitro and in vivo based on immunofluorescence staining (200× magnification). (c) The protein levels of TRAF3 in vitro and in vivo based on western blotting assay. All data are expressed as the mean ± *SD* (n = 5). $^{*}P < .05$ compared with control group or sham group; $^{\#}P < .05$ compared with 120 min of reoxygenation or 90 min of reperfusion group

of ischaemia and 90 min of reperfusion in vivo compared with sham group. However, the expression levels of TRAF3 were clearly reduced with further prolongation of reoxygenation or reperfusion time compared with 120 min of reoxygenation in vitro and 90 min of reperfusion in vivo.

3.5 | MiR-29b-3p adjusted TRAF3 signal pathway

As shown in Figure 5a,b, the protein levels of p-TAK1, NF-κB (p65), and BAX were clearly increased, and Bcl-2 expression levels were depressed in H/R groups in vitro and II/R groups in vivo compared with control group or sham group. However, with further prolongation of reoxygenation or reperfusion time, the expression levels of p-TAK1, NF-κB (p65), and BAX were decreased, and Bcl-2 expression levels were increased compared with 120 min of reoxygenation in vitro or 90 min of reperfusion in vivo. The data in Figure 5c,d showed that the mRNA levels of IL-1β, IL-6, and TNF-α were the highest levels at 120 min of reoxygenation in vitro or 90 min of reperfusion in vivo compared with control group or sham group, which were y reduced from 720 to 1,440 min of reoxygenation or reperfusion

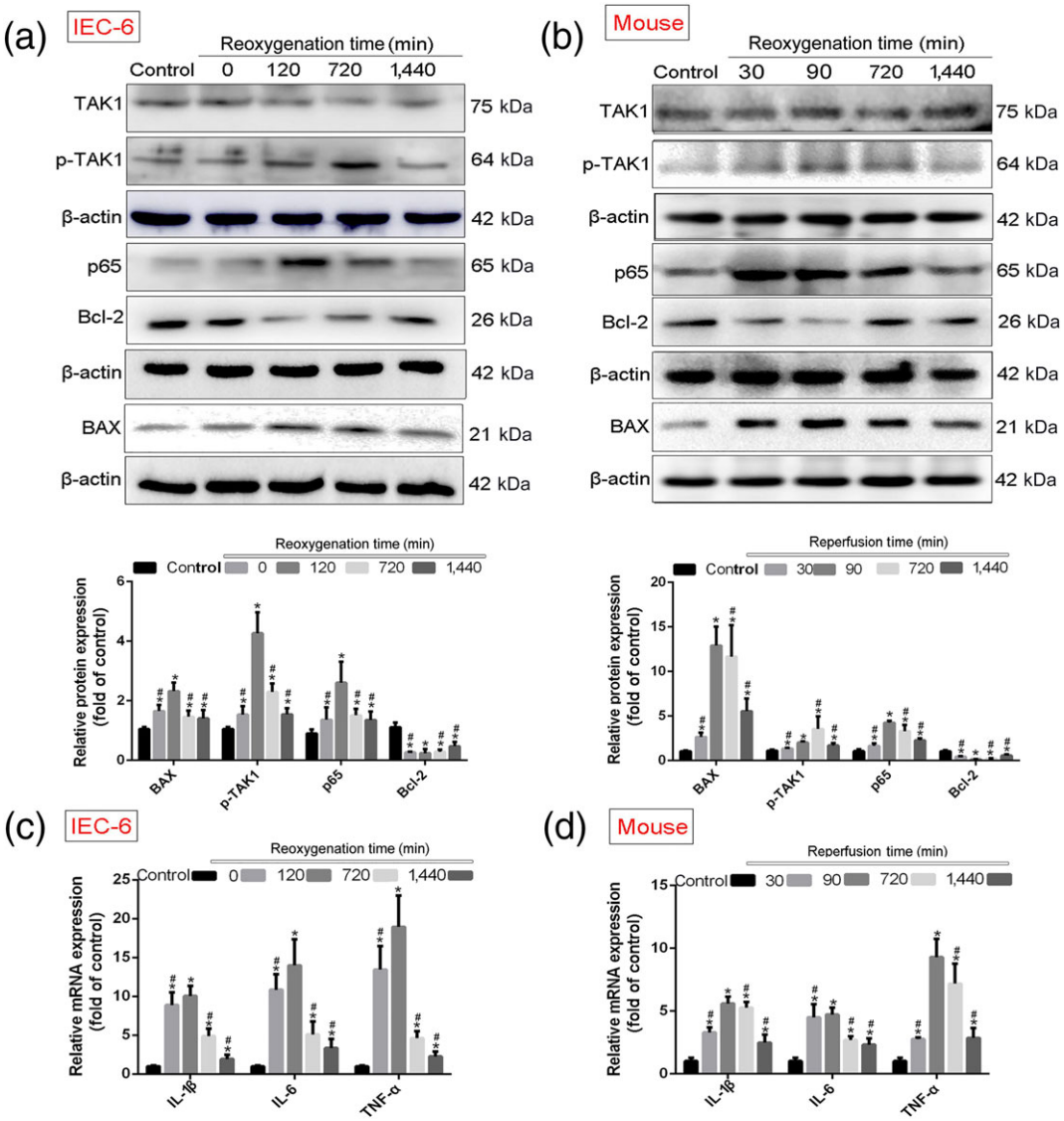

FIGURE 5 MiR-29b-3p inhibited TRAF3 signal in vitro and in vivo. Protein and RNA samples were extracted from IEC-6 cells subjected to hypoxia for 4 hr, reoxygenation for 0, 120, 720, and 1,440 min, and intestinal tissues of mice suffered from ischaemia for 45 min, reperfusion for 30, 90, 720, and 1,440 min using the kits. Then the protein levels were examined by western blotting assay, and the mRNA levels of were tested by real-time PCR assay. (a, b) The protein levels of TAK1, p-TAK1, NF-κB (p65), BAX, and Bcl-2 in IEC-6 cells and mice. (c, d) The mRNA levels of IL-1β, IL-6, and TNF-α in vitro and in vivo. All data are expressed as the mean ± *SD* ($n = 5$). $^{*}P < .05$ compared with control group or sham group; $^{\#}P < .05$ compared with 120 min of reoxygenation or 90 min of reperfusion group

compared with 120 min of reoxygenation in vitro or 90 min of reperfusion in vivo.

3.6 | Overexpression of miR-29b-3p alleviated H/R-caused injury in vitro

As shown in Figure 6a, the viability and morphology of cells showed little change compared with control group after transfection with miR-29b-3p mimic, suggesting that miR-29b-3p mimic did not produce side effects. The data in Figure 6b showed that after transfection with miR-29b-3p mimic, the expression level of miR-29b-3p in IEC-6 cells was clearly increased, indicating that miR-29b-3p mimic was successfully transfected into the cells. As shown in Figure 6c, after transfection, cell apoptosis was decreased, and the expression level of miR-29b-3p was increased, and TRAF3 mRNA level was decreased compared with H/R group (Figure 6d). In addition, the data in Figure 6e–g indicated that the protein levels of TRAF3, p-TAK1, NF-κB (p65), and BAX were decreased, Bcl-2 expression level was increased, and inflammation was reduced compared with H/R group after transfected with miR-29b-3p mimic. Hence, overexpression of miR-29b-3p protected against II/R injury via inhibiting TRAF3 signalling.

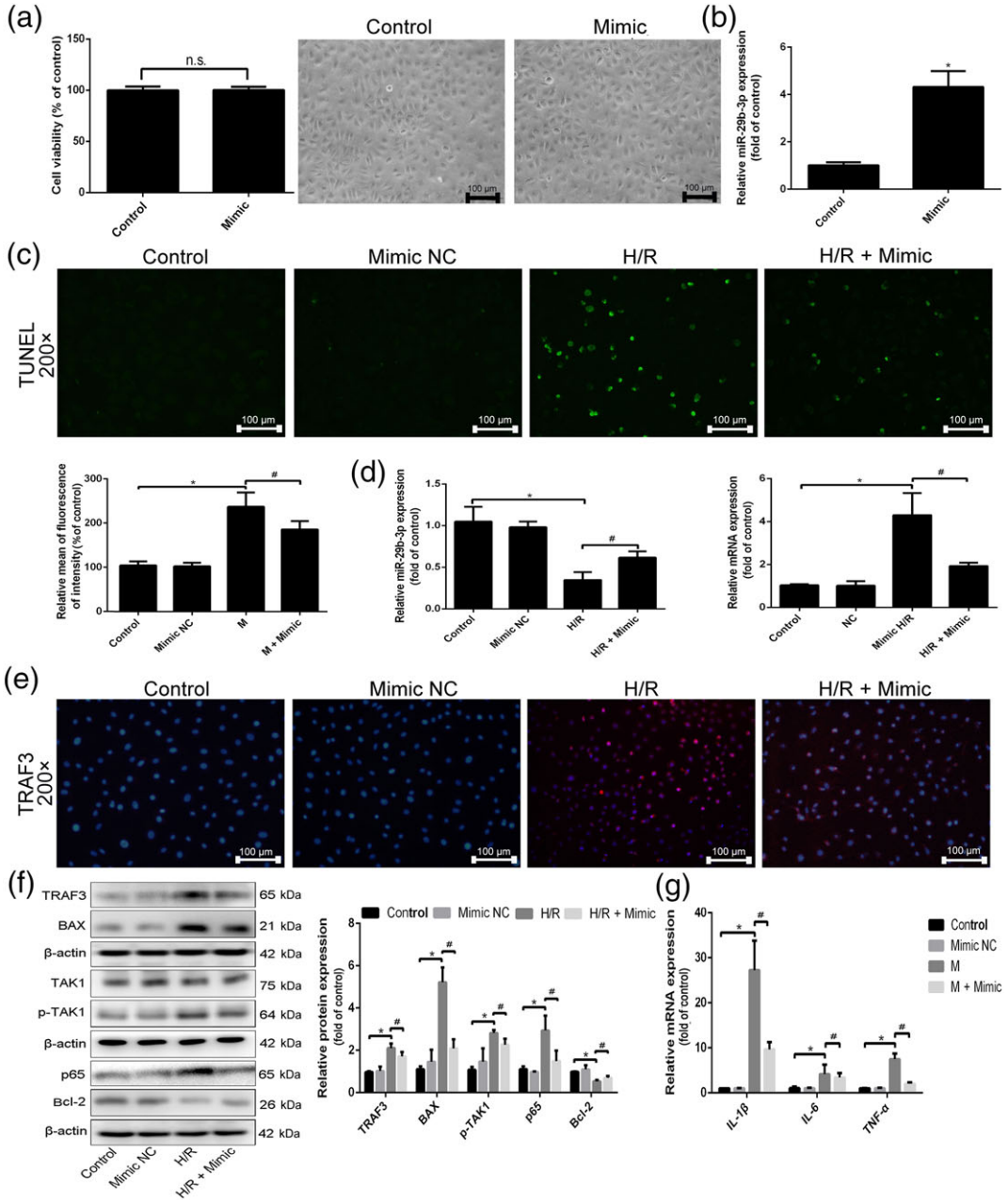

FIGURE 6 Overexpression of miR-29b-3p alleviated H/R-caused injury. IEC-6 cells were seeded and transfected with miR-29b-3p mimic in antibiotic-free cell medium, and the relevant indicators were detected after transfection for 24 hr. (a) The viability and morphology of IEC-6 cells after transfected with miR-29b-3p mimic. (b) The expression level of miR-29b-3p in IEC-6 cells after transfected with miR-29b-3p mimic. (c) Cell apoptosis in IEC-6 cells after transfection of miR-29b-3p mimic. (d) The expression level of miR-29b-3p and TRAF3 mRNA level after transfected with miR-29b-3p mimic in IEC-6 cells. (e) The protein level of TRAF3 after transfection of miR-29b-3p mimic in IEC-6 cells based on immunofluorescence staining (200× magnification). (f) The protein levels of the TRAF3, TAK1, p-TAK1, NF-κB (p65), BAX, and Bcl-2 after transfection of miR-29b-3p mimic in IEC-6 cells. (g) The mRNA levels of IL-1β, IL-6, and TNF-α after transfection of miR-29b-3p mimic in IEC-6 cells. All data are expressed as the mean ± *SD* ($n = 5$). $^{*}P < .05$ compared with control group; $^{\#}P < .05$ compared with H/R group; n.s., no significance

3.7 | TRAF3 siRNA mitigated H/R-caused injury in vitro

The data in Figure 7a showed that after transfection with TRAF3 siRNA, the viability and morphology of cells showed little change compared with control group, indicating that TRAF3 siRNA showed no side effects in the cells following transfection. As shown in Figure 7b, the mRNA level of TRAF3 in IEC-6 cells was decreased after transfection with TRAF3 siRNA, suggesting that TRAF3 siRNA was successfully transfected into the cells. As shown in Figure 7c, the numbers of apoptotic cells were reduced, and TRAF3 mRNA level was significantly decreased after transfection with TRAF3 siRNA, compared with H/R group (Figure 7d). Moreover, the data in Figure 7e–g indicated that after transfection with TRAF3 siRNA, the

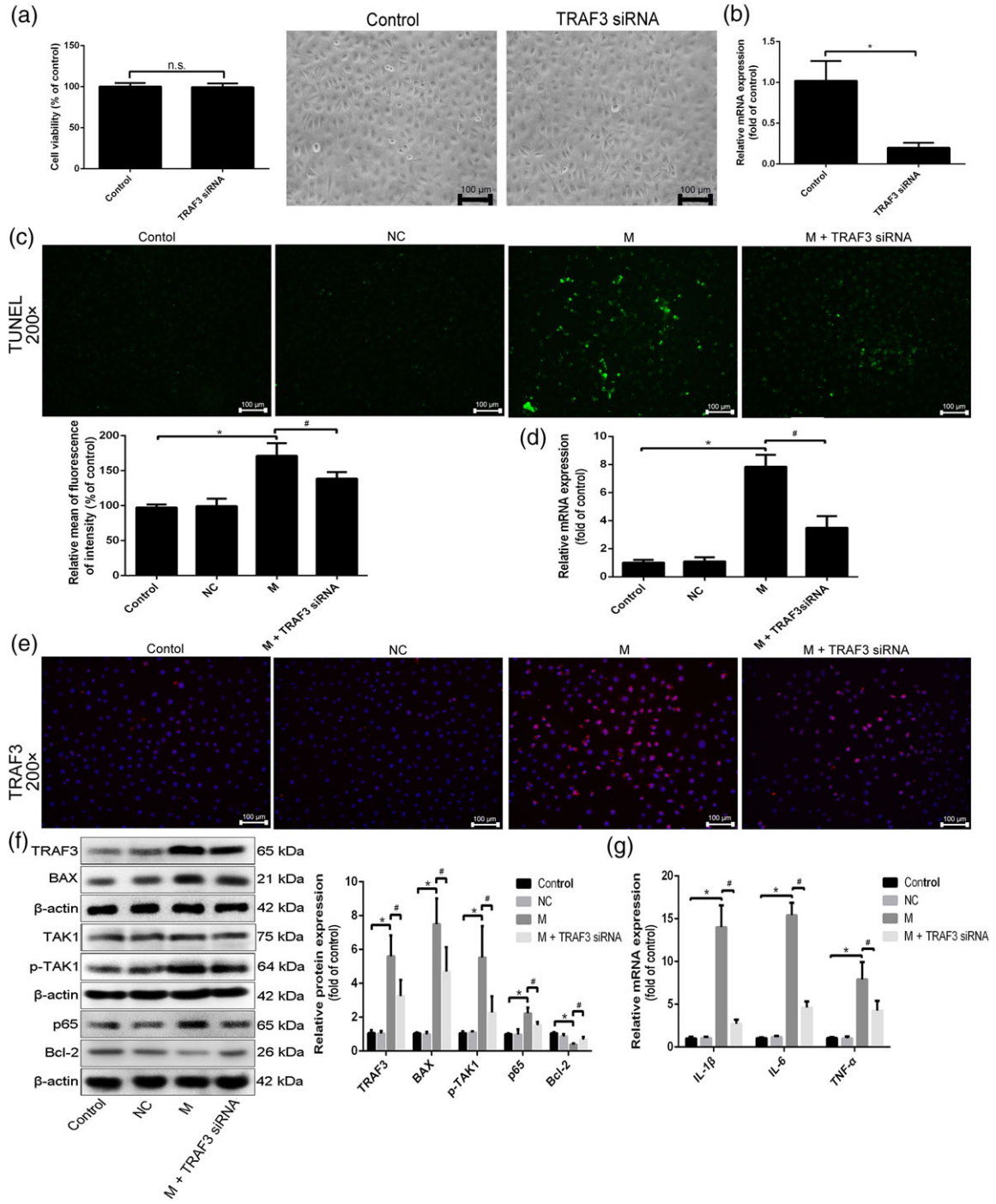

FIGURE 7 Blockade of TRAF3 mitigated H/R-caused injury in cells. IEC-6 cells were transfected with TRAF3 siRNA in antibiotic-free cell medium for 24 hr. (a) The viability and morphology of IEC-6 cells after transfected with TRAF3 siRNA. (b) The expression level of TRAF3 in cells after transfected with TRAF3 siRNA. (c) Cell apoptosis after transfection of TRAF3 siRNA in IEC-6 cells. (d) The mRNA level of TRAF3 after transfected with TRAF3 siRNA in IEC-6 cells. (e) The protein level of TRAF3 after transfection of TRAF3 siRNA in IEC-6 cells by immunofluorescence staining (200× magnification). (f) The protein levels of TRAF3, TAK1, p-TAK1, NF-κB (p65), BAX, and Bcl-2 after transfection of TRAF3 siRNA in IEC-6 cells by western blotting assay. (g) The mRNA levels of IL-1β, IL-6, and TNF-α after transfection of TRAF3 siRNA in IEC-6 cells. All data are expressed as the mean ± *SD* (n = 5). $^{*}P < .05$, significantly different from control group; $^{\#}P < .05$, significantly different from H/R group; n.s., not significant

expression levels of TRAF3, p-TAK1, NF-κB (p65), and BAX were decreased, Bcl-2 expression level was increased, and inflammation reaction was clearly inhibited compared with H/R group. Hence, blockade of TRAF3 reduced II/R injury.

4 | DISCUSSION

II/R damage caused by bowel infarction, strangulation, severe hypotension, and shock is a frequent and clinically devastating condition

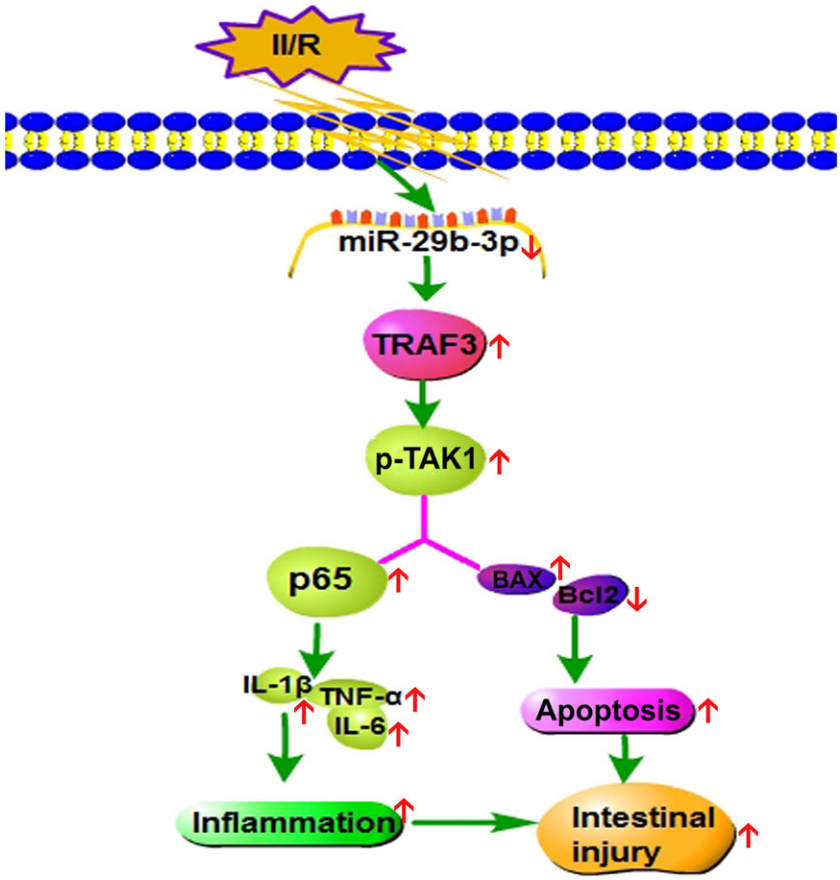

FIGURE 8 Diagram of the mechanisms of miR-29b-3p in controlling II/R damage. MiR-29b-3p decreased the expression levels of p-TAK1 and p65 via targeting TRAF3 to alleviate apoptosis and inflammation caused by II/R

with high morbidity and mortality. II/R can cause intestinal mucosal injury and ultimately lead to bacterial translocation, sepsis, multiple organ failure, and eventually death (Ceulemans et al., 2017; Goldsmith et al., 2012; Mallick, Yang, Winslet, & Seifalian, 2004). As mentioned above, apoptosis and inflammation are important mechanisms associated with II/R injury. TUNEL staining is one major method to detect cell apoptosis, and pro-inflammatory factors including IL-1β, IL-6, and TNF-α can reflect inflammatory response (Y. Li, Wen, et al., 2017; Y. Li, Xu, et al., 2017; Zu, Zhou, Che, & Zhang, 2018). In this study, our results showed that the numbers of apoptotic cells and the mRNA levels of IL-1β, IL-6, and TNF-α were significantly increased after 4 hr of hypoxia and 120 min of reoxygenation in IEC-6 cells and ischaemia for 45 min and reperfusion for 90 min in mice compared with control group or sham group, which were reduced with the prolongation of reoxygenation or reperfusion time compared with 120 min of reoxygenation in vitro or reperfusion for 90 min in vivo.

Previous studies have shown that miRNAs can control the pathological process of II/R injury (Y. Hu et al., 2018; Z. Li et al., 2018; Y. Li, Wen, et al., 2017; Y. Li, Xu, et al., 2017). In addition, some miRNAs including miR-375 and miR-371 have been confirmed as the markers for clinical diagnosis and treatment of diseases (Piano et al., 2019; Salvatori et al., 2018). Circulating miRNA-375 can be considered as a biomarker for active Kaposi's sarcoma in AIDS patients (Piano et al., 2019). The MiR-371 family can be used as the plasma biomarkers for monitoring undifferentiated and potentially malignant human pluripotent stem cells (Salvatori et al., 2018). Besides, some groups have reported that miR-29b-3p plays important roles in cell apoptosis, inflammation, and oxidative stress (Jing et al., 2018; H. Wang et al., 2017; Xing et al., 2014; Zhang et al., 2017). MiR-29 can be used as a clinical marker of disease. Thus, miR-29c has been suggested as a diagnostic and therapeutic biomarker in gastric carcinogenesis, for patients with gastric cancer (Han et al., 2015) and serum miR-29 has served as the biomarker for Parkinson's disease (Bai et al., 2017). MiR-29b-3p, a member of miR-29 family, has important roles in clinical practice. Pan et al. (2019) have found low expression level of miR-29b-3p in serum of multiple myeloma patients. Circulating basal level of miR-29b-3p can predict the outcome of patients with metastatic colorectal cancer treated with bevacizumab (Ulivi et al., 2018). However, no papers have reported the functions of miR-29b-3p on II/R injury. In this study, we explored the possible clinical application of miR-29b-3p in II/R injury and found that the expression levels of miR-29b-3p were significantly decreased in H/R and II/R groups compared with control group in vitro and sham group in vivo. Moreover, we found that TRAF3 showed putative binding sites with miR-29b-3p. In co-transfection experiments, we found that, after a single transfection of TRAF3 overexpression plasmid in cells, TRAF3 expression was significantly increased compared with control group. However, after co-transfection of miR-29b-3p mimic and TRAF3 overexpression plasmid, TRAF3 expression levels were clearly reduced compared with single transfection of TRAF3 overexpression plasmid, suggesting that miR-29b-3p directly targeted TRAF3.

II/R injury-induced SIRS and MODS can lead to death in patients (L. Liu et al., 2018; Perez-Chanona, Mühlbauer, & Jobin, 2014; Rivers et al., 2001). As demonstrated in this study, II/R injury aggravated intestinal mucosa inflammation and apoptosis which can eventually cause SIRS and MODS. In order to further explore the roles of miR-29b-3p in reducing II/R damage, transfection test of miR-29b-3p mimic was carried out. The results showed that miR-29b-3p reduced II/R damage through inhibiting TRAF3 signal via decreasing the expression levels of TRAF3, p-TAK1, and NF-κB (p65) and increasing Bcl-2 expression level to suppress apoptosis and inflammation. MiR-29b-3p/TRAF3 signal can be considered as one new target for the research and development of innovative drugs to treat II/R injury.

TRAF3 can regulate the functions of some types of receptors with multiple roles in a variety of signalling pathways (Shi & Sun, 2018; Yi, Lin, Stunz, & Bishop, 2014). Gu et al. (2015) have shown that TRAF3 plays important roles in modulating apoptosis and inflammation. However, its effects on II/R injury have not been reported. Previous studies have shown that **intestinal fatty acid-binding protein** has emerged as a valuable marker for the diagnosis of intestinal damage at an early stage (Khadaroo et al., 2014; Thuijls et al., 2011). Schellekens et al. (2018) have proposed that smooth muscle protein 22 can be considered as a potential marker of transmural intestinal ischaemia in patients. In this study, the results showed that the expression levels of TRAF3 were clearly increased in H/R and II/R groups compared with control group in vitro and sham group in vivo. The transfection with TRAF3 siRNA showed that TRAF3 aggravated II/R injury via activating TAK1 phosphorylation, increasing NF-κB level to promote inflammation, up-regulating BAX expression, and down-regulating Bcl-2 expression to promote apoptosis. From these results, we suggest that TRAF3 played important roles in regulating II/R injury in our model. However, whether TRAF3 can be used as a biomarker for clinical diagnosis or treatment of II/R injury remains to be further explored.

In conclusion, our findings in this paper provided novel insights into the molecular mechanism(s) underlying the effects of miR-29b-3p on II/R injury by means of TRAF3 signalling (Figure 8). This pathway should be developed as an effective drug target for clinical diagnosis and treatment of II/R injury.

ACKNOWLEDGEMENTS

This work was financially supported by National Natural Science Foundation of China (81872921), the Key Research and Development Project of Liaoning Province (2017225090), the Science and Technology Innovation Project of Dalian, China (2018J128N083), and the Project of Leading Talents of Dalian, and LiaoNing Revitalization Talents Program (XLYC1802121).

CONFLICT OF INTEREST

The authors declare no conflicts of interest.

AUTHOR CONTRIBUTIONS

Y.D. and J.P. designed the experiments and wrote the manuscript. Y.D., Z.M., X.H., and Y.X. performed the animal and cell experiments. L.Y., L.X., and Y.Q. performed the quantitative real-time PCR and western blotting assays. Y.D. and Y.X. performed the gene transfection experiments. J.P. edited the manuscript.

DECLARATION OF TRANSPARENCY AND SCIENTIFIC RIGOUR

This Declaration acknowledges that this paper adheres to the principles for transparent reporting and scientific rigour of preclinical research as stated in the *BJP* guidelines for Design & Analysis, Immunoblotting and Immunochemistry, and Animal Experimentation, and as recommended by funding agencies, publishers and other organisations engaged with supporting research.

ORCID

Jinyong Peng https://orcid.org/0000-0002-6265-2667

REFERENCES

Alexander, S. P. H., Kelly, E., Marrion, N. V., Peters, J. A., Faccenda, E., Harding, S. D., … CGTP Collaborators. (2017). The Concise Guide to PHARMACOLOGY 2017/18: Other ion channels. *British Journal of Pharmacology*, *174*, S195–S207. https://doi.org/10.1111/bph.13881

Alexander, S. P. H., Peters, J. A., Kelly, E., Marrion, N. V., Faccenda, E., Harding, S. D., … CGTP Collaborators. (2017). The Concise Guide to PHARMACOLOGY 2017/18: Ligand-gated ion channels. *British Journal of Pharmacology*, *174*, S130–S159. https://doi.org/10.1111/bph.13879

Alexander, S. P. H., Striessnig, J., Kelly, E., Marrion, N. V., Peters, J. A., Faccenda, E., … CGTP Collaborators. (2017). The Concise Guide to PHARMACOLOGY 2017/18: Voltage-gated ion channels. *British Journal of Pharmacology*, *174*, S160–S194. https://doi.org/10.1111/bph.13884

Bai, X., Tang, Y., Yu, M., Wu, L., Liu, F., Ni, J., … Wang, J. (2017). Downregulation of blood serum microRNA 29 family in patients with Parkinson's disease. *Scientific Reports*, *7*, 5411. https://doi.org/10.1038/s41598-017-03887-3

Ceulemans, L. J., Verbeke, L., Decuypere, J. P., Farré, R., De Hertogh, G., Lenaerts, K., … Pirenne, J. (2017). Farnesoid X receptor activation attenuates intestinal ischemia reperfusion injury in rats. *PLoS ONE*, *12*, e0169331. https://doi.org/10.1371/journal.pone.0169331

Curtis, M. J., Alexander, S., Cirino, G., Docherty, J. R., George, C. H., Giembycz, M. A., … Ahluwalia, A. (2018). Experimental design and analysis and their reporting II: Updated and simplified guidance for authors and peer reviewers. *British Journal of Pharmacology*, *175*, 987–993. https://doi.org/10.1111/bph.14153

Duranti, S., Vivo, V., Zini, I., Milani, C., Mangifesta, M., Anzalone, R., … Turroni, F. (2018). Bifidobacterium bifidum PRL2010 alleviates intestinal ischemia/reperfusion injury. *PLoS ONE*, *13*, e0202670. https://doi.org/10.1371/journal.pone.0202670

Enyindah-Asonye, G., Li, Y., Xin, W., Singer, N. G., Gupta, N., Fung, J., & Lin, F. (2017). CD6 receptor regulates intestinal ischemia/reperfusion-induced injury by modulating natural IgM-producing B1a cell self-renewal. *The Journal of Biological Chemistry*, *292*, 661–671. https://doi.org/10.1074/jbc.M116.749804

Feinman, R., Deitch, E. A., Watkins, A. C., Abungu, B., Colorado, I., Kannan, K. B., … Xu, D. Z. (2010). HIF-1 mediates pathogenic inflammatory responses to intestinal ischemia-reperfusion injury. *American Journal of Physiology. Gastrointestinal and Liver Physiology*, *299*, G833–G843. https://doi.org/10.1152/ajpgi.00065.2010

Feng, D., Yao, J., Wang, G., Li, Z., Zu, G., Li, Y., … Tian, X. (2017). Inhibition of p66Shc-mediated mitochondrial apoptosis via targeting prolyl-isomerase Pin1 attenuates intestinal ischemia/reperfusion injury in rats. *Clinical Science (London, England)*, *131*, 759–773. https://doi.org/10.1042/CS20160799

Filpa, V., Carpanese, E., Marchet, S., Pirrone, C., Conti, A., Rainero, A., … Porta, G. (2017). Nitric oxide regulates homeoprotein OTX1 and OTX2 expression in the rat myenteric plexus after intestinal ischemia-reperfusion injury. *American Journal of Physiology. Gastrointestinal and Liver Physiology*, *312*, G374–G389. https://doi.org/10.1152/ajpgi.00386.2016

Goldsmith, J. R., Perez-Chanona, E., Yadav, P. N., Whistler, J., Roth, B., & Jobin, C. (2012). Sa1939 intestinal epithelial cell (IEC)-derived Mu-Opioid signaling is protective against ischemia reperfusion (I/R) induced injury. *Gastroenterology*, *142*, 351–364.

Gu, H., Yu, J., Dong, D., Zhou, Q., Wang, J. Y., & Yang, P. (2015). The miR-322-TRAF3 circuit mediates the pro-apoptotic effect of high glucose on neural stem cells. *Toxicological Sciences*, *144*, 186–196. https://doi.org/10.1093/toxsci/kfu271

Han, T. S., Hur, K., Xu, G., Choi, B., Okugawa, Y., Toiyama, Y., … Yang, H. K. (2015). MicroRNA-29c mediates initiation of gastric carcinogenesis by directly targeting ITGB1. *Gut*, *64*, 203–214. https://doi.org/10.1136/gutjnl-2013-306640

Harding, S. D., Sharman, J. L., Faccenda, E., Southan, C., Pawson, A. J., Ireland, S., … NC-IUPHAR. (2018). The IUPHAR/BPS Guide to PHARMACOLOGY in 2018: Updates and expansion to encompass the new guide to IMMUNOPHARMACOLOGY. *Nucleic Acids Research*, *46*(D1), D1091–D1106. https://doi.org/10.1093/nar/gkx1121

He, X., Zheng, Y., Liu, S., Shi, S., Liu, Y., He, Y., … Zhou, X. (2018). MiR-146a protects small intestine against ischemia/reperfusion injury by down-regulating TLR4/TRAF6/NF-κB pathway. *Journal of Cellular Physiology*, *233*, 2476–2488. https://doi.org/10.1002/jcp.26124

Hu, J., Zhu, X. H., Zhang, X. J., Wang, P. X., Zhang, R., Zhang, P., … Li, H. (2016). Targeting TRAF3 signaling protects against hepatic ischemia/reperfusions injury. *Journal of Hepatology*, *64*, 146–159. https://doi.org/10.1016/j.jhep.2015.08.021

Hu, Y., Tao, X., Han, X., Xu, L., Yin, L., Sun, H., … Peng, J. (2018). MicroRNA-351-5p aggravates intestinal ischaemia/reperfusion injury through the targeting of MAPK13 and sirtuin-6. *British Journal of Pharmacology*, *175*, 3594–3609. https://doi.org/10.1111/bph.14428

Ikeda, H., Suzuki, Y., Suzuki, M., Koike, M., Tamura, J., Tong, J., … Itoh, G. (1998). Apoptosis is a major mode of cell death caused by ischaemia and ischaemia/reperfusion injury to the rat intestinal epithelium. *Gut*, *42*, 530–537. https://doi.org/10.1136/gut.42.4.530

Impellizzeri, D., Cordaro, M., Campolo, M., Gugliandolo, E., Esposito, E., Benedetto, F., … Navarra, M. (2016). Anti-inflammatory and antioxidant effects of flavonoid-rich fraction of bergamot juice (BJe) in a mouse model of intestinal ischemia/reperfusion injury. *Frontiers in Pharmacology*, *7*, 203.

Inoue, J., Ishida, T., Tsukamoto, N., Kobayashi, N., Naito, A., Azuma, S., & Yamamoto, T. (2000). Tumor necrosis factor receptor-associated factor (TRAF) family: Adapter proteins that mediate cytokine signaling. *Experimental Cell Research*, *254*, 14–24. https://doi.org/10.1006/excr.1999.4733

Jing, X., Yang, J., Jiang, L., Chen, J., & Wang, H. (2018). MicroRNA-29b regulates the mitochondria-dependent apoptotic pathway by targeting Bax in doxorubicin cardiotoxicity. *Cellular Physiology and Biochemistry*, *48*, 692–704. https://doi.org/10.1159/000491896

Khadaroo, R. G., Fortis, S., Salim, S. Y., Streutker, C., Churchill, T. A., & Zhang, H. (2014). I-FABP as biomarker for the early diagnosis of acute mesenteric ischemia and resultant lung injury. *PLoS ONE*, *9*, e115242. https://doi.org/10.1371/journal.pone.0115242

Kilkenny, C., Browne, W., Cuthill, I. C., Emerson, M., & Altman, D. G. (2010). Animal research: Reporting in vivo experiments: The ARRIVE guidelines. *British Journal of Pharmacology*, *160*, 1577–1579. https://doi.org/10.1111/j.1476-5381.2010.00872.x

Langsch, S., Baumgartner, U., Haemmig, S., Schlup, C., Schäfer, S. C., Berezowska, S., … Vassella, E. (2016). miR-29b mediates NF-κB signaling in KRAS-induced non-small cell lung cancers. *Cancer Research*, *76*, 4160–4169. https://doi.org/10.1158/0008-5472.CAN-15-2580

Li, Y., Wen, S., Yao, X., Liu, W., Shen, J., Deng, W., … Liu, K. (2017). MicroRNA-378 protects against intestinal ischemia/reperfusion injury via a mechanism involving the inhibition of intestinal mucosal cell apoptosis. *Cell Death & Disease*, *8*, e3127. https://doi.org/10.1038/cddis.2017.508

Li, Y., Xu, B., Xu, M., Chen, D., Xiong, Y., Lian, M., … Lin, Y. (2017). 6-Gingerol protects intestinal barrier from ischemia/reperfusion-induced damage via inhibition of p38 MAPK to NF-κB signalling. *Pharmacological Research*, *119*, 137–148. https://doi.org/10.1016/j.phrs.2017.01.026

Li, Z., Wang, G., Feng, D., Zu, G., Li, Y., Shi, X., … Tian, X. (2018). Targeting the miR-665-3p-ATG4B-autophagy axis relieves inflammation and apoptosis in intestinal ischemia/reperfusion. *Cell Death & Disease*, *9*, 483. https://doi.org/10.1038/s41419-018-0518-9

Liu, L., Yao, J., Li, Z., Zu, G., Feng, D., Li, Y., … Tian, X. (2018). miR-381-3p knockdown improves intestinal epithelial proliferation and barrier function after intestinal ischemia/reperfusion injury by targeting nurr1. *Cell Death & Disease*, *9*, 411. https://doi.org/10.1038/s41419-018-0450-z

Liu, X. H., Yang, Y. W., Dai, H. T., Cai, S. W., Chen, R. H., & Ye, Z. Q. (2015). Protective role of adiponectin in a rat model of intestinal ischemia reperfusion injury. *World Journal of Gastroenterology*, *21*, 13250–13258. https://doi.org/10.3748/wjg.v21.i47.13250

Liu, Z., Jiang, J., Yang, Q., Xiong, Y., Zou, D., Yang, C., … Zhan, H. (2016). MicroRNA-682-mediated downregulation of PTEN in intestinal epithelial cells ameliorates intestinal ischemia-reperfusion injury. *Cell Death & Disease*, *7*, e2210. https://doi.org/10.1038/cddis.2016.84

Mallick, I. H., Yang, W., Winslet, M. C., & Seifalian, A. M. (2004). Ischemia-reperfusion injury of the intestine and protective strategies against injury. *Digestive Diseases and Sciences*, *49*, 1359–1377. https://doi.org/10.1023/B:DDAS.0000042232.98927.91

Matsuo, S., Chaung, A., Liou, D., Wang, P., & Yang, W. L. (2018). Inhibition of ubiquitin-activating enzyme protects against organ injury after intestinal ischemia-reperfusion. *American Journal of Physiology. Gastrointestinal and Liver Physiology*, *315*, G283–G292. https://doi.org/10.1152/ajpgi.00024.2018

McGrath, J. C., & Lilley, E. (2015). Implementing guidelines on reporting research using animals (ARRIVE etc.): New requirements for publication in BJP. *British Journal of Pharmacology*, *172*, 3189–3193. https://doi.org/10.1111/bph.12955

Pan, Y., Zhang, Y., Liu, W., Huang, Y., Shen, X., Jing, R., … Chen, H. (2019). LncRNA H19 over-expression induces bortezomib resistance in multiple myeloma by targeting MCL-1 via miR-29b-3p. *Cell Death & Disease*, *10*, 106. https://doi.org/10.1038/s41419-018-1219-0

Perez-Chanona, E., Mühlbauer, M., & Jobin, C. (2014). The microbiota protects against ischemia/reperfusion-induced intestinal injury through

nucleotide-binding oligomerization domain-containing protein 2 (NOD2) signaling. *The American Journal of Pathology*, *184*, 2965–2975. https://doi.org/10.1016/j.ajpath.2014.07.014

Piano, M. A., Gianesello, L., Grassi, A., Del Bianco, P., Mattiolo, A., Cattelan, A. M., … Calabrò, M. L. (2019). Circulating miRNA-375 as a potential novel biomarker for active Kaposi's sarcoma in AIDS patients. *Journal of Cellular and Molecular Medicine*, *23*, 1486–1494. https://doi.org/10.1111/jcmm.14054

Qu, F., Xiang, Z., Zhou, Y., Qin, Y., & Yu, Z. (2017). Tumor necrosis factor receptor-associated factor 3 from Anodontawoodiana is an important factor in bivalve immune response to pathogen infection. *Fish & Shellfish Immunology*, *71*, 151–159. https://doi.org/10.1016/j.fsi.2017.10.004

Rehei, A. L., Zhang, L., Fu, Y. X., Mu, W. B., Yang, D. S., Liu, Y., … Younusi, A. (2018). MicroRNA-214 functions as an oncogene in human osteosarcoma by targeting TRAF3. *European Review for Medical and Pharmacological Sciences*, *22*, 5156–5164. https://doi.org/10.26355/eurrev_201808_15711

Rivers, E., Nguyen, B., Havstad, S., Ressler, J., Muzzin, A., Knoblich, B., … Early Goal-Directed Therapy Collaborative Group. (2001). Early goal-directed therapy in the treatment of severe sepsis and septic shock. *The New England Journal of Medicine*, *345*, 1368–1377. https://doi.org/10.1056/NEJMoa010307

Salvatori, D. C. F., Dorssers, L. C. J., Gillis, A. J. M., Perretta, G., van Agthoven, T., Gomes Fernandes, M., … Looijenga, L. H. J. (2018). The microRNA-371 family as plasma biomarkers for monitoring undifferentiated and potentially malignant human pluripotent stem cells in teratoma assays. *Stem Cell Reports*, *11*, 1493–1505. https://doi.org/10.1016/j.stemcr.2018.11.002

Schellekens, D. H. S. M., Reisinger, K. W., Lenaerts, K., Hadfoune, M., Olde Damink, S. W., Buurman, W. A., … Derikx, J. P. M. (2018). SM22 a plasma biomarker for human transmural intestinal ischemia. *Annals of Surgery*, *268*, 120–126. https://doi.org/10.1097/SLA.0000000000002278

Shi, J. H., & Sun, S. C. (2018). Tumor necrosis factor receptor-associated factor regulation of nuclear factor κB and mitogen-activated protein kinase pathways. *Frontiers in Immunology*, *9*, 1849. https://doi.org/10.3389/fimmu.2018.01849

Sun, H., Zhong, D., Wang, C., Sun, Y., Zhao, J., & Li, G. (2018). MiR-298 exacerbates ischemia/reperfusion injury following ischemic stroke by targeting Act1. *Cellular Physiology and Biochemistry*, *48*, 528–539. https://doi.org/10.1159/000491810

Tackett, J. J., Gandotra, N., Bamdad, M. C., Muise, E. D., & Cowles, R. A. (2019). Potentiation of serotonin signaling protects against intestinal ischemia and reperfusion injury in mice. *Neurogastroenterology and Motility*, *31*, e13498. https://doi.org/10.1111/nmo.13498

Thuijls, G., van Wijck, K., Grootjans, J., Derikx, J. P., van Bijnen, A. A., Heineman, E., … Poeze, M. (2011). Early diagnosis of intestinal ischemia using urinary and plasma fatty acid binding proteins. *Annals of Surgery*, *253*, 303–308. https://doi.org/10.1097/SLA.0b013e318207a767

Ulivi, P., Canale, M., Passardi, A., Marisi, G., Valgiusti, M., Frassineti, G. L., … Scarpi, E. (2018). Circulating plasma levels of miR-20b, miR-29b and miR-155 as predictors of bevacizumab efficacy in patients with metastatic colorectal cancer. *International Journal of Molecular Sciences*, *19*, 307. https://doi.org/10.3390/ijms19010307

Wang, H., An, X., Yu, H., Zhang, S., Tang, B., Zhang, X., & Li, Z. (2017). MiR-29b/TET1/ZEB2 signaling axis regulates metastatic properties and epithelial-mesenchymal transition in breast cancer cells. *Oncotarget*, *8*, 102119–102133. https://doi.org/10.18632/oncotarget.22183

Wen, S. H., Li, Y., Li, C., Xia, Z. Q., Liu, W. F., Zhang, X. Y., … Liu, K. X. (2012). Ischemic postconditioning during reperfusion attenuates intestinal injury and mucosal cell apoptosis by inhibiting JAK/STAT signaling activation. *Shock*, *38*, 411–419. https://doi.org/10.1097/SHK.0b013e3182662266

Xing, L. N., Wang, H., Yin, P. H., Liu, Y. J., Chi, Y. F., Wang, Y. M., & Peng, W. (2014). Reduced mir-29b-3p expression up-regulate CDK6 and contributes to IgA nephropathy. *International Journal of Clinical and Experimental Medicine*, *7*, 5275–5281.

Yao, S., Tang, B., Li, G., Fan, R., & Cao, F. (2016). miR-455 inhibits neuronal cell death by targeting TRAF3 in cerebral ischemic stroke. *Neuropsychiatric Disease and Treatment*, *12*, 3083–3092. https://doi.org/10.2147/NDT.S121183

Yi, Z., Lin, W. W., Stunz, L. L., & Bishop, G. A. (2014). Roles for TNF-receptor associated factor 3 (TRAF3) in lymphocyte functions. *Cytokine & Growth Factor Reviews*, *25*, 147–156. https://doi.org/10.1016/j.cytogfr.2013.12.002

Zhang, S., Wang, Z., Zhu, J., Xu, T., Zhao, Y., Zhao, H., … Yao, J. (2017). Carnosic acid alleviates BDL-induced liver fibrosis through miR-29b-3p-mediated inhibition of the high-mobility group box 1/toll-like receptor 4 signaling pathway in rats. *Frontiers in Pharmacology*, *8*, 976.

Zheng, Y., Pan, C., Chen, M., Pei, A., Xie, L., & Zhu, S. (2019). miR-29a ameliorates ischemic injury of astrocytes in vitro by targeting the water channel protein aquaporin 4. *Oncology Reports*, *41*, 1707–1717.

Zhou, S., Lei, D., Bu, F., Han, H., Zhao, S., & Wang, Y. (2018). MicroRNA-29b-3p targets SPARC gene to protect cardiocytes against autophagy and apoptosis in hypoxic-induced H9c2 cells. *Journal of Cardiovascular Translational Research*. https://doi.org/10.1007/s12265-018-9858-1

Zhou, W., Yao, J., Wang, G., Chen, Z., Li, Z., Feng, D., … Tian, X. (2017). PKCζ phosphorylates TRAF2 to protect against intestinal ischemia-reperfusion-induced injury. *Cell Death & Disease*, *8*, e2935. https://doi.org/10.1038/cddis.2017.310

Zu, G., Zhou, T., Che, N., & Zhang, X. (2018). Salvianolic acid A protects against oxidative stress and apoptosis induced by intestinal ischemia-reperfusion injury through activation of Nrf2/HO-1 pathways. *Cellular Physiology and Biochemistry*, *49*, 2320–2332.

SUPPORTING INFORMATION

Additional supporting information may be found online in the Supporting Information section at the end of the article.

How to cite this article: Dai Y, Mao Z, Han X, et al. MicroRNA-29b-3p reduces intestinal ischaemia/reperfusion injury via targeting of TNF receptor-associated factor 3. *Br J Pharmacol*. 2019;176:3264–3278. https://doi.org/10.1111/bph.14759